

Learning Purified Feature Representations from Task-irrelevant Labels

Yinghui Li^{1*}, Ruiyang Liu², Chen Wang², Li Yangning¹, Ning Ding^{1,2}, Hai-Tao Zheng¹

¹Tsinghua Shenzhen International Graduate School, Tsinghua University

²Department of Computer Science and Technology, Tsinghua University

{liyinghu20, lry20, wchen20}@mails.tsinghua.edu.cn

Abstract

Learning an empirically effective model with generalization using limited data is a challenging task for deep neural networks. In this paper, we propose a novel learning framework called *Purified Learning* to exploit task-irrelevant features extracted from task-irrelevant labels when training models on small-scale datasets. Particularly, we purify feature representations by using the expression of task-irrelevant information, thus facilitating the learning process of classification. Our work is built on solid theoretical analysis and extensive experiments, which demonstrate the effectiveness of Purified Learning. According to the theory we proved, Purified Learning is model-agnostic and doesn't have any restrictions on the model needed, so it can be combined with any existing deep neural networks with ease to achieve better performance. The source code of this paper will be available in the future for reproducibility.

Introduction

With sufficient manually annotated training samples, deep neural networks could automatically perform feature extraction and achieve unprecedented performances on various classification tasks (Gu et al. 2018). However, collecting and annotating adequate training data is an extremely time-consuming and expensive process, leading that in many instances the training samples are insufficient and even noisy (Zhang et al. 2020). Under this circumstance, the performance of deep models always drops gravely on most classification tasks (Ajiboye, Abdullah-Arshah, and Hongwu 2015; Prusa, Khoshgoftaar, and Seliya 2015). The essential reason for the phenomenon is that the goal of “minimizing the empirical risk” is not reliable when the training data is inadequate (Wang et al. 2020), as a result, deep neural models will easily overfit the training data. Therefore, training effective deep neural models with remarkable generalization performance on small training samples is of great practical importance in terms of vastly expanding the scalability of deep learning methods.

Many techniques have been developed to tackle the issue. Some approaches directly expanding training samples (Cubuk et al. 2018; Bowles et al. 2018; Chen et al. 2020; Zhang et al. 2014; Shinohara 2016a) to alleviate the shortage of annotated data, but may be limited because expansion based on small-scale training samples is only of theoretical significance and not operability. On the other hand, previous studies also attempt to break through the limitation of a specific dataset and find training samples in a broad sense. Based on this motivation, transfer learning (Wang and Hebert 2016; Luo et al. 2017) exploits knowledge from additional datasets with relevant content and labels, achieving remarkable improvements on the target task. However, they only achieve good results when labels are relevant enough since irrelevant labels could bring out massive negative transfer (Weiss, Khoshgoftaar, and Wang 2016; Rosenstein et al. 2005). And to date, there have been few studies that use task-irrelevant features to improve the performance of deep learning models. In this paper, we argue that while transferring task-relevant labels from other datasets, task-irrelevant labels could also be utilized to improve the generalization of classification on small datasets without conflicts.

Consider a running example in computer vision: facial expression recognition a.k.a FER, which aims at constructing a model to accurately predict the expression of unseen facial pictures. In this task, it is obvious that *smiling* is a task-relevant feature, while *hair color* is a proper task-irrelevant one. Assume we have a small-scale FER dataset, which is often the case in real-world deep learning tasks. Since the training dataset is extremely small, it is unavoidable that the distribution of task-irrelevant features i.e., *hair color* have non-negligible bias. For example, most people with black hair might be labeled as *happy* and people with white hair are exactly labeled as *sad*. This kind of bias is a ubiquitous problem when training samples are insufficient, which has already been observed in many previous works (Tommasi et al. 2017; Torralba and Efros 2011).

As we mentioned before, the task-irrelevant features create a substantial barrier for the learning process due to the problem of “minimizing the empirical risk”, which leads to the models inevitably overfit hair features. As a result, the performance of the trained models on unseen facial expression samples are severely affected. An intuitive method to address the issue is to make use of massive related facial information from other facial datasets by transfer learning, but as we mentioned, there would be severe negative transfer when using irrelevant facial information (*hair color*). Our methodology is motivated by the predicament, which is to utilize vast samples that has task-irrelevant features to tackle

*The first three authors have equal contribution.

this problem.

In this paper, we propose Purified Learning to explore task-irrelevant features from large-scale and easily available datasets with the same content as the training set. By minimizing the Wasserstein distance between the distribution of representation extracted from samples with a fixed task-irrelevant label and that from the entire dataset, we reduce the influence of task-irrelevant features. This suppression of task-irrelevant features plays a “two negatives make a positive” role that further highlights the representation ability of task-relevant features and finally improve model generalization. In summary, in this paper we make three-fold contributions:

- We theoretically prove that task-irrelevant labels can help to extract helpful features while only small-scale training dataset is available.
- We propose Purified Learning, which use task-irrelevant labels to facilitate the learning process, finally derive a purified feature representation that has minimum task-irrelevant components.
- We conduct extensive experiments and analyses on FER and digit recognition. Results show that we achieve state-of-the-art performance on digit recognition task when the training set is small.

Theory

Unreliability of Minimizing Empirical Risk

For a learning task \mathcal{T} , a training sample set including I labeled instances $D_{train} = \{(x_1, y_1), (x_2, y_2), \dots, (x_I, y_I)\}$ is given. Let $p(x, y)$ be the ground-truth joint probability distribution of sample x and label y . We denote the space of input instance by \mathcal{X} , and the space of task labels by \mathcal{Y} , $x \in \mathcal{X}$ and $y \in \mathcal{Y}$. The goal of deep learning is to learn a model $f(x; \theta) : \{\mathcal{X}; \Theta\} \rightarrow \mathcal{Y}$ parameterized by $\theta \in \Theta$ from training data to minimize the expected risk, i.e.,

$$\min_f R(f) = \int \mathcal{L}(f(x; \theta), y) dp(x, y), \quad (1)$$

where \mathcal{L} refers to a certain loss function, e.g., mean squared error or cross entropy loss.

As $p(x, y)$ is unknown, the most classical approach is to approximate the expected risk by minimizing the empirical risk (Vapnik 1991; Mohri, Rostamizadeh, and Talwalkar 2012), which is the average of sample losses over the training set D_{train} of I samples:

$$\min_f R_{emp}(f) = \frac{1}{I} \sum_{i=1}^I \mathcal{L}(y_i, f(x_i)), \text{ s.t. } (x_i, y_i) \in D_{train}. \quad (2)$$

However, obviously that when the distribution of the training sample differs greatly from the true distribution $p(x, y)$, especially when I is small, the empirical risk $R_{emp}(f)$ may then be far from being a good approximation of the expected risk $R(f)$, which makes it no longer reliable (Wang et al. 2020). The bias of task-irrelevant features in the training dataset is one of the main causes of the deviation between training data distribution and $p(x, y)$. We believe that

weakening the impact of task-irrelevant features will help train models with better generalization performance, which requires introducing knowledge of task-irrelevant features from samples with task-irrelevant labels.

Task-Irrelevant Labels

Task-irrelevant features are defined as the features irrelevant to the target task, and task-relevant features are features relevant to the target task. For example, hair color is a task-irrelevant feature for the FER task. Correspondingly, if samples from some irrelevant tasks contain the same content but different labels with the target task, the labels are termed as task-irrelevant labels, and the samples are termed as task-irrelevant samples. Note that in practice, the task irrelevance of a label is related to the performance loss of transfer learning, not by human judgments. The more negative the transferring effect is, the more irrelevant the label is.

For a specific target task, and a dataset with task-irrelevant labels, $S = \{(x, y_{tir})\}$, we denote the feature space by \mathcal{X} , $x \in \mathcal{X}$, and the label space of task-irrelevant labels by \mathcal{Y} , $Y = \{y_1, y_2, y_3, \dots, y_n\}$, $y_{tir} \in Y$. Input x contains some features that are task-relevant, denoted by x_{tr} and the distribution of x_{tr} in S is denoted by \mathbb{S} .

We select all samples whose $y_{tir} = y_1$ from S , denoted by S_{y_1} :

$$S_{y_1} = \{(x, y_{tir}) | y_{tir} = y_1, (x, y_{tir}) \in S\}, \quad (3)$$

and the distribution of x_{tr} in S_{y_1} is denoted by \mathbb{S}_{y_1} . Since y_{tir} is irrelevant with x_{tr} , we have:

$$\mathbb{S} = \mathbb{S}_{y_1}. \quad (4)$$

In deep models, the feature extractor f_e is used to extract representation r from input data. Here, R and R_{y_1} are extracted from S and S_{y_1} ,

$$\begin{aligned} R &= \{(r, y_{tir}) | r = f_e(x), (x, y_{tir}) \in S\} \\ R_{y_1} &= \{(r, y_{tir}) | r = f_e(x), (x, y_{tir}) \in S_{y_1}\}. \end{aligned} \quad (5)$$

Similarly, the distributions of r in R and R_{y_1} are denoted by \mathbb{R} and \mathbb{R}_{y_1} .

Under ideal conditions, a good extractor only extracts task-relevant features, so $\mathbb{R} = \mathbb{R}_{y_1}$. However, in reality, the extractor inevitably extracts task-irrelevant features and leads to $\mathbb{R} \neq \mathbb{R}_{y_1}$. The greater the difference between \mathbb{R} and \mathbb{R}_{y_1} , the more the extractor is influenced by task-irrelevant features. To reduce this difference, Purified Learning aims to minimize the divergence between these two distributions,

$$\min(\text{WD}(\mathbb{R}, \mathbb{R}_{y_1})), \quad (6)$$

WD is Wasserstein distance that is used to measure the divergence between two distributions.

Theoretical Analysis of Purified Learning

Motivated by (Shen et al. 2017), we provide a theoretical analysis of Wasserstein distance’s efficacy and its generalization bound here. The classification model is divided into two parts, a classifier f_c , and a feature extractor f_e . After sending an input instance to the extractor f_e , we get a

representation r , so $f_e : \mathcal{X} \rightarrow \mathcal{R}$ where \mathcal{R} denotes and $f_c : \mathcal{R} \rightarrow \mathcal{Y}$ where \mathcal{Y} is the space of labels as defined before.

H is a hypothesis class that for every $h \in H$, $h : \mathcal{R} \rightarrow \mathcal{Y}$ and h is K -Lipschitz continuous. In neural networks, we limit the scale of the weights so that f_c is K -Lipschitz continuous and $f_c \in H$. For every distribution \mathbb{D} on \mathcal{X} , the corresponding distribution of representation is denoted by \mathbb{R} , $\mathbb{R} = f_e(\mathbb{D})$. The difference of h_1 and h_2 ($h_1, h_2 \in H$) on \mathbb{R} are defined by:

$$\epsilon_{\mathbb{R}}(h_1, h_2) = \mathbb{E}_{r \sim \mathbb{R}} [||h_1(r) - h_2(r)||]. \quad (7)$$

Similarly,

$$\epsilon_{\mathbb{D}}(h_1 \circ f_e, h_2 \circ f_e) = \mathbb{E}_{x \sim \mathbb{D}} [||h_1(f_e(x)) - h_2(f_e(x))||]. \quad (8)$$

Theorem 1: For representation distributions $\mathbb{R}_1, \mathbb{R}_2$ on \mathcal{R} , and $h_1, h_2 \in H$. Then the following holds:

$$\epsilon_{\mathbb{R}_1}(h_1, h_2) \leq \epsilon_{\mathbb{R}_2}(h_1, h_2) + 2K \cdot \text{WD}(\mathbb{R}_1, \mathbb{R}_2). \quad (9)$$

Proof. We first prove that $|h_1 - h_2|$ is $2K$ -Lipschitz continuous. Using the triangle inequality, we have:

$$\begin{aligned} ||h_1(r) - h_2(r)|| &\leq ||h_1(r) - h_1(r')|| + ||h_1(r') - h_2(r)|| \\ &\leq ||h_1(r) - h_1(r')|| + ||h_1(r') - h_2(r')|| \\ &\quad + ||h_2(r) - h_2(r')||, \end{aligned} \quad (10)$$

thus,

$$\begin{aligned} &||h_1(r) - h_2(r)|| - ||h_2(r') - h_2(r')|| \\ &\leq ||h_1(r) - h_1(r')|| + ||h_1(r) - h_2(r')||, \end{aligned} \quad (11)$$

then, because both h_1 and h_2 are K -Lipschitz continuous,

$$\begin{aligned} &\frac{||h_1(r) - h_2(r)|| - ||h_2(r') - h_2(r')||}{\rho(r, r')} \\ &\leq \frac{||h_1(r) - h_1(r')|| + ||h_2(r) - h_2(r')||}{\rho(r, r')} \leq 2K. \end{aligned} \quad (12)$$

Thus, $|h_1 - h_2|$ is $2K$ -Lipschitz continuous. Then we have:

$$\begin{aligned} &\epsilon_{\mathbb{R}_1}(h_1, h_2) - \epsilon_{\mathbb{R}_2}(h_1, h_2) \\ &= \mathbb{E}_{r \in \mathbb{R}_1} [||h_1(r) - h_2(r)||] - \mathbb{E}_{r \in \mathbb{R}_2} [||h_1(r) - h_2(r)||] \\ &\leq \sup_{\|f\|_L \leq 2K} \mathbb{E}_{r \sim \mathbb{R}_1} [f(r)] - \mathbb{E}_{r \sim \mathbb{R}_2} [f(r)] \\ &= 2K \cdot \text{WD}(\mathbb{R}_1, \mathbb{R}_2). \end{aligned} \quad (13)$$

So far, **Theorem 1** is proven.

Next, we give the upper bound of generalization error by Wasserstein distance. Denoting the ideal classifier for a specific classification task by f_c^* , both f_c and f_c^* are K -Lipschitz continuous. To achieve the optimal performance, f_c needs to approach the ideal classifier f_c^* . So the error of f_c on distribution \mathbb{R} is defined as $\gamma_{\mathbb{R}}(f_c)$:

$$\gamma_{\mathbb{R}}(f_c) = \epsilon_{\mathbb{R}}(f_c, f_c^*). \quad (14)$$

For two distribution of input instances, denoted by \mathbb{D}_1 and \mathbb{D}_2 , their corresponding representation distributions are \mathbb{R}_1 and \mathbb{R}_2 . According to Theorem 1, we have:

$$\epsilon_{\mathbb{R}_1}(f_c, f_c^*) \leq \epsilon_{\mathbb{R}_2}(f_c, f_c^*) + 2K \cdot \text{WD}(\mathbb{R}_1, \mathbb{R}_2), \quad (15)$$

thus,

$$\gamma_{\mathbb{R}_1}(f_c) \leq \gamma_{\mathbb{R}_2}(f_c) + 2K \cdot \text{WD}(\mathbb{R}_1, \mathbb{R}_2). \quad (16)$$

Correspondingly,

$$\gamma_{\mathbb{D}_1}(f_c \circ f_e) \leq \gamma_{\mathbb{D}_2}(f_c \circ f_e) + 2K \cdot \text{WD}(\mathbb{R}_1, \mathbb{R}_2). \quad (17)$$

WD is Wasserstein distance that is used to measure the divergence between two distributions. Thus, for an unknown test distribution \mathbb{D}_1 , minimizing error on \mathbb{D}_1 can be divided into two goals. The first one is to minimize error on the given training sample distribution \mathbb{D}_2 . The second is to minimize the Wasserstein distance between \mathbb{R}_1 and \mathbb{R}_2 . Since \mathbb{R}_1 is unknown, we need to approximate it using another dataset. According to unreliability of empirical risk, we need another large-scale dataset to approximate the distribution of \mathbb{R}_1 . Large-scale data ensures that the distribution is more close to the testing set. In practice, we use the feature distribution R of S , mentioned in Sec. to do the approximation.

Framework of Purified Learning

Purified Learning focuses on exploiting the knowledge contained in task-irrelevant labels from auxiliary samples and transferring it to the target task. With this knowledge, we measure the influence of task-irrelevant features, and then use the adversarial learning method based on Wasserstein distances to limit such influence during feature extraction. In this way, original extract features is purified, increasing the percentage of task-relevant features. Generally, the framework is divided into three parts: a feature extractor f_e , a linear classifier f_c and an additional discriminator f_d , as shown in Figure 1. We denote the dataset of the target task by \mathcal{S}_{tgt} , and the task-irrelevant dataset by \mathcal{S}_{src} . Note that Purified Learning is a theoretically validation framework, the extractor, discriminator and classifier are all flexible and have multiple choices. A practice choice is to set them according to performance. To utilize both \mathcal{S}_{tgt} and \mathcal{S}_{src} , two optimization goals are set according to Sec. .

Goal 1: Empirical Risk Minimization

For training sample x and label y , $(x, y) \in \mathcal{S}_{tgt}$, the classification probability $p = \text{softmax}(f_c(f_e(x)))$, and the classification loss is calculated by cross-entropy loss, which is consistent with the loss in empirical risk.

$$\begin{aligned} \mathcal{L}_{\text{classification}} = & \\ & - \sum_{x, y \in \mathcal{S}_{tgt}} y * \log(\text{softmax}(f_c(f_e(x)))) . \end{aligned} \quad (18)$$

Goal 1 is the empirical risk minimization that we minimize the classification error so that the model learns the knowledge contained in the samples of \mathcal{S}_{tgt} . However, the generalization ability of the model trained on Goal 1 depends heavily on the consistency of the training data distribution and the real data distribution as we discussed before, which is usually hard to achieve on a small dataset. Thus, a new optimization goal should be imported to utilize large-scale task-relevant or task-irrelevant data to reduce this bias.

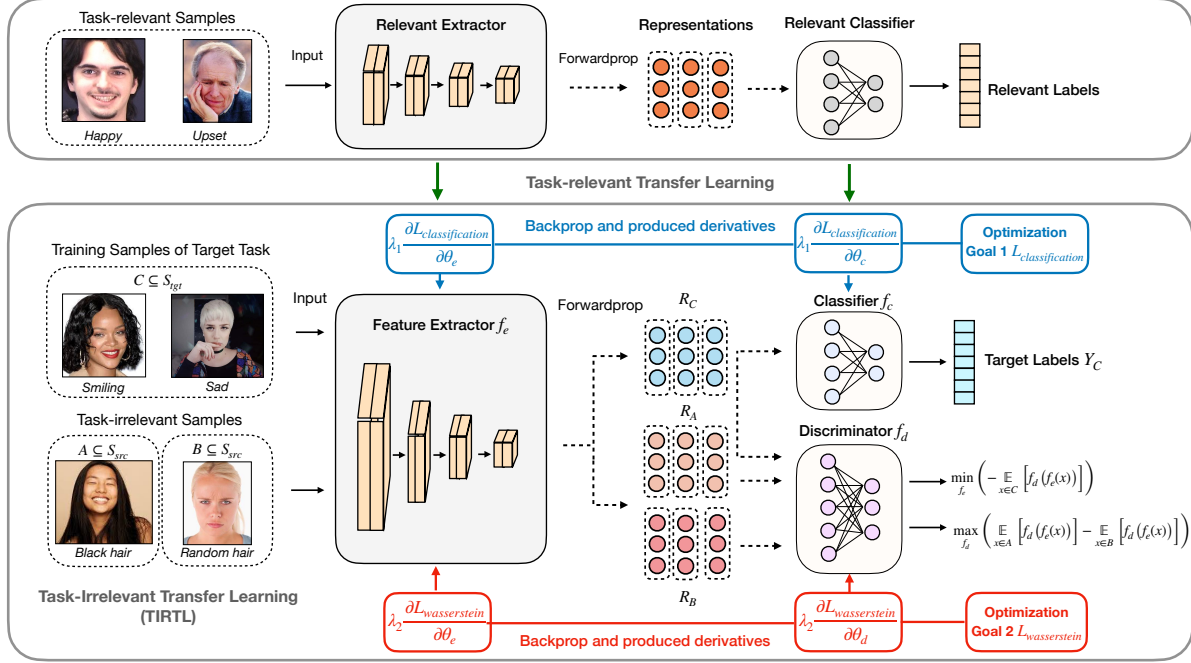


Figure 1: An overview of Purified Learning framework, which contains a feature extractor, a discriminator and a classifier. The top of the diagram shows how it can be easily combined with existing models that use task-relevant information, see Appendix A for details.

Goal 2: Wasserstein Distance Minimization

This goal aims to minimize the Wasserstein distance between \mathbb{R}_{y_1} and \mathbb{R} as Equation 6, and it is necessary to estimate the two distributions by sampling. For \mathcal{S}_{src} , we randomly select two groups of samples, one from samples with a specific task-irrelevant label y_1 in \mathcal{S}_{src} , denoted by A , and the other from the entire \mathcal{S}_{src} , denoted by B .

For A and B , the representations extracted by f_e are denoted by R_A, R_B :

$$\begin{aligned} R_A &= \{f_e(x) | x \in A\} \\ R_B &= \{f_e(x) | x \in B\}. \end{aligned} \quad (19)$$

When the sizes of A and B are large enough, the representation distributions of R_A and R_B , denoted by \mathbb{R}_A and \mathbb{R}_B , are used as reasonable estimations of \mathbb{R}_{y_1} and \mathbb{R} . Thus, Equation 6 is rewritten as:

$$\min(\text{WD}(\mathbb{R}_A, \mathbb{R}_B)). \quad (20)$$

We substitute the WD with Wasserstein's Kantorovich-Rubinstein duality form,

$$\min_{f_e} \sup_{\|f_d\|_{L \leq 1}} \left(\mathbb{E}_{x \in A} [f_d(f_e(x))] - \mathbb{E}_{x \in B} [f_d(f_e(x))] \right). \quad (21)$$

Inspired by WGAN (Arjovsky, Chintala, and Bottou 2017), Equation 21 could be divided into two steps. Firstly, the discriminator f_d is trained by:

$$\max_{f_d} \left(\mathbb{E}_{x \in A} [f_d(f_e(x))] - \mathbb{E}_{x \in B} [f_d(f_e(x))] \right). \quad (22)$$

Secondly, we select a group of training samples, C , from training dataset of target task \mathcal{S}_{tgt} . The feature representations extracted by f_e are denoted by R_C ,

$$R_C = \{f_e(x) | x \in C\}, \quad (23)$$

then, the extractor f_e is trained by:

$$\min_{f_e} \left(- \mathbb{E}_{x \in C} [f_d(f_e(x))] \right), \quad (24)$$

and the corresponding Wasserstein loss is:

$$\mathcal{L}_{\text{wasserstein}} = - \frac{1}{\|C\|} \sum_{x \in C} [f_d(f_e(x))], \quad (25)$$

where $\|C\|$ is the size of the sample group C .

Combining $\mathcal{L}_{\text{classification}}$ and $\mathcal{L}_{\text{wasserstein}}$, the complete loss function is written as follows, where λ_1 and λ_2 are weighting factors:

$$\mathcal{L}_{\text{Purify Learning}} = \lambda_1 \mathcal{L}_{\text{classification}} + \lambda_2 \mathcal{L}_{\text{wasserstein}}. \quad (26)$$

In practice, the training algorithm is shown in Alg. 1.

Experiments

We conduct extensive experiments to evaluate the effectiveness of our proposed Purified Learning in terms of improving the model generalization. A series of subsidiary experiments are carried out for deep analysis and some of the results are reported in Appendix D.

Feature Extractor	Train → Test Dataset	Goal 1 Only	TL (Hair Color)	MTL (Hair Color)	AMTL (Hair Color)	PL (Hair Color)
AlexNet	ck+ → mmi	35.91	38.28	33.73	34.57	37.61
	ck+ → oulu	34.75	25.54	33.08	33.15	38.31
	mmi → ck+	56.36	44.97	57.09	57.94	61.45
	mmi → oulu	22.12	19.89	23.66	28.73	22.61
	oulu → ck+	55.03	54.42	54.67	43.52	59.64
	oulu → mmi	39.46	40.00	40.30	28.33	45.36
	Average	40.61	37.18	40.42	37.37	44.16
ResNet34	ck+ → mmi	50.42	46.54	46.54	44.35	50.42
	ck+ → oulu	50.94	54.29	47.24	43.75	51.78
	mmi → ck+	65.33	68.73	66.18	64.61	69.21
	mmi → oulu	44.87	46.13	40.96	42.15	42.43
	oulu → ck+	73.45	73.33	72.93	66.18	80.12
	oulu → mmi	54.13	49.01	51.43	41.99	54.30
	Average	56.52	56.34	54.21	50.51	58.04
VggNet19	ck+ → mmi	45.53	41.10	37.10	33.05	45.53
	ck+ → oulu	56.66	44.52	32.24	47.66	57.22
	mmi → ck+	65.33	62.30	64.61	57.82	66.79
	mmi → oulu	45.08	32.17	46.69	40.20	46.76
	oulu → ck+	76.73	71.27	72.12	31.88	78.91
	oulu → mmi	45.03	43.68	40.00	20.24	51.43
	Average	55.73	49.17	48.79	38.48	57.77

Table 1: Results (Accuracy %) on FER task, where TL refers to transfer learning, MTL refers to multi-task learning, AMTL refers to adversarial multi-task learning, and PL refers to Purified Learning. $ck+ \rightarrow mmi$ means model is trained on $ck+$ and tested on mmi dataset. TL (Hair Color) means using *hair color* label in transfer learning.

Experimental Setup

Model As mentioned before, the framework of Purified Learning consists of three parts: a feature extractor, a linear classifier, and a discriminator. The discriminator consists of four fully connected layers. The linear classifier is a fully connected layer with the number of neurons depending on the specific task. The flexibility of Purified Learning enables that various mainstream models can be embed as feature extractor.

Evaluation Metrics To evaluate the results of model generalization, the cross-dataset test results are taken as evaluation metrics. This is based on a reasonable assumption: the training set and the real data distribution are different, and the unseen test set is sampled from the real data distribution, so there exists a gap between the distribution of test data and that of training data. Therefore, the higher the accuracy in our test means the better the generalization performance of the model.

Hyperparameters We implement all experiments without data augmentation. The model is trained by an SGD optimizer with an initial learning rate of 0.001, the momentum of 0.9, StepLR(step size is 7), and γ of 0.1. We apply widely used classification models (e.g ResNet) as a feature extractor and set the output dimension of the penultimate layer to 128. The classifier is a fully connected layer and the output dimension is equal to the number of classes (7 for FER and 10 for digit recognition). The discriminator consists of four fully connected layers with 512, 256, 10, 1 nodes, the discriminator is trained using an Adam with the same learning rate, and a weight limit 0.1.

In addition, the step ratio of n_2 in Alg.1 is 3. The factors λ_1 and λ_2 are both 1. We use batch size 32 in FER, and 128 in digit recognition. All results are obtained after the model has been trained for 50 epochs.

Experiments on Facial Expression Recognition

In this part, we compare Purified Learning with some methods related to our work on the FER task. These methods are briefly described below, and their implementation details are shown in Appendix B:

- **Goal 1 Only**: As an empirical baseline, we use labeled training data to train the model with the optimization goal 1 only.
- **Transfer learning** : We use the hair color recognition task to pre-train the network, and then fine-tune on FER task.
- **Multi-task learning** : We train FER and hair color recognition tasks using a shared feature extractor.
- **Adversarial multi-task learning**: We add a gradient inversion layer for the hair color recognition task on the multi-task learning method above.

Datasets and Feature Extractors In FER experiments, we use small-scale datasets, including $ck+$ (Lucey et al. 2010), $oulu$ (Zhao et al. 2011) and mmi (Pantic et al. 2005) for cross-dataset evaluation. We select AlexNet (Krizhevsky, Sutskever, and Hinton 2012), VggNet19 (Simonyan and Zisserman 2015) and ResNet34 (He et al. 2016) as feature extractors. The datasets used in the experiment are detailed in Appendix C.

Algorithm 1 Algorithm of Purified Learning.

Require: target training sample set \mathcal{S}_{tgt} ; task-irrelevant sample set \mathcal{S}_{src} ; learning rate for discriminator α_1 ; learning rate for feature extractor and classifier α_2 ; batch size m ; Iteration numbers n_1, n_2 .

Notation: function fitted by the feature extractor, f_e ; function fitted by the classifier, f_c ; function fitted by the discriminator, f_d .

```

1: Initialize feature extractor, linear classifier, discriminator with random weights  $\theta_e, \theta_c, \theta_d$ .
2: for  $n_1$  steps do
3:   Sample minibatch  $A = \{a^{(i)}\}_{i=1}^m$  from  $\mathcal{S}_{src}$  with a fixed task-irrelevant label.
4:   Sample minibatch  $B = \{b^{(i)}\}_{i=1}^m$  from  $\mathcal{S}_{src}$  with random task-irrelevant labels.
5:    $g_d \leftarrow \nabla_d (\frac{1}{m} \sum_{i=1}^m (f_d(f_e(b^{(i)})) - f_d(f_e(a^{(i)})))$ 
6:    $\theta_d \leftarrow \theta_d + \alpha_1 Adam(\theta_d, g_d)$ 
7:   for  $n_2$  steps do
8:     Sample minibatch  $C = \{x^{(i)}, y^{(i)}\}_{i=1}^m$  from  $\mathcal{S}_{tgt}$ .
9:     Goal 1:
10:     $g_c \leftarrow \nabla_c (\sum_{i=1}^m (-y^{(i)} \cdot \log(f_c(f_e(x^{(i)}))))$ 
11:     $\theta_c \leftarrow \theta_c - \alpha_2 SGD(\theta_c, g_c)$ 
12:     $g_e \leftarrow \nabla_e (\sum_{i=1}^m (-y^{(i)} \cdot \log(f_c(f_e(x^{(i)}))))$ 
13:     $\theta_e \leftarrow \theta_e - \alpha_2 SGD(\theta_e, g_e)$ 
14:     Goal 2:
15:     $g_e \leftarrow \nabla_e (\frac{1}{m} \sum_{i=1}^m (-f_d(f_e(x^{(i)}))))$ 
16:     $\theta_e \leftarrow \theta_e - \alpha_2 SGD(\theta_e, g_e)$ 

```

We use 224×224 resolution for all RGB pictures and preprocess them through MTCNN (Zhang et al. 2016) for alignment. More importantly, the *hair color* label in CelebA (Liu et al. 2015) is regarded as task-irrelevant label. Therefore, we select samples with fixed *hair color* labels and samples randomly selected from CelebA, and then using Purified Learning on them.

Results Table 1 is the comparison between Purified Learning and baseline methods, which shows that our method achieves better results in 14 of 18 cross-dataset tests.

Since hair color is not relevant to FER, it leads to negative transfer for transfer learning methods including transfer learning, multi-task learning and adversarial multi-task learning (lower accuracy even than Goal 1 Only in most cases). The performance of the adversarial multi-task learning is the worst because it requires training samples with both task label and task-irrelevant label. However, in our experiments, the training samples are only annotated with task labels, and the task-irrelevant labels are from additional samples. By contrast, Purified Learning is able to make use of the knowledge from task-irrelevant labels, so it improves the accuracy of Goal 1 only, thus successfully resolving negative transfer and improving the generalization performance of the model.

Train → Test Dataset	Feature Extractor	Goal 1 Only	DANN	PL (Background Color)
MNIST → SVHN	DenseNet121	13.85	10.64	16.44
	EfficientNet	22.99	13.99	33.74
	MobileNetV2	20.06	11.35	22.11
	ResNet18	15.01	12.00	18.83
	SeNet	15.44	10.69	18.22
	ShuffleNetV2	14.29	11.98	20.72
	VggNet11	19.50	13.79	25.71
MNIST → MNIST-M	Average	17.31	12.06	22.25
	DenseNet121	25.26	14.28	35.21
	EfficientNet	40.78	38.71	57.64
	MobileNetV2	29.77	21.75	48.76
	ResNet18	25.10	22.54	37.64
	SeNet	17.24	15.83	39.71
	ShuffleNetV2	27.96	20.34	47.65
MNIST → CelebA	VggNet11	39.18	42.09	48.98
	Average	29.33	25.08	45.08

Table 2: Results (Accuracy %) on digit recognition task.

Experiments on Digit Recognition

In this part, we evaluate Purified Learning on Digit Recognition task. In this experiment, we add another baseline, DANN (Ajakan et al. 2014), a domain transfer framework based on adversarial multi-task learning. DANN is currently the state-of-the-art method of transferring from MNIST to MNIST-M¹. Since we use small-scale training set, our accuracy is lower than original paper. The model details of DANN and the experiment results to verify the correctness of the DANN we implement are shown in Appendix B and Appendix D, respectively.

Feature Extractor	Train → Test Dataset	Goal 1 Only	PL (Smiling)	PL (Hair Color)
AlexNet	ck+ → mmi	35.91	32.38	37.61
	ck+ → oulu	34.75	33.91	38.31
	mmi → ck+	56.36	35.39	61.45
	mmi → oulu	22.12	18.77	22.61
	oulu → ck+	55.03	49.33	59.64
	oulu → mmi	39.46	38.45	45.36
ResNet34	Average	40.61	34.71	44.16
	ck+ → mmi	50.42	47.89	50.42
	ck+ → oulu	50.94	50.31	51.78
	mmi → ck+	65.33	65.70	69.21
	mmi → oulu	44.87	39.22	42.43
	oulu → ck+	73.45	73.70	80.12
VggNet19	oulu → mmi	54.13	51.43	54.30
	Average	56.52	54.71	58.04
	ck+ → mmi	45.53	40.47	45.53
	ck+ → oulu	56.66	42.99	57.22
	mmi → ck+	65.33	63.64	66.79
	mmi → oulu	45.08	44.59	46.76
DenseNet121	oulu → ck+	76.73	75.03	78.91
	oulu → mmi	45.03	50.59	51.43
	Average	55.73	52.89	57.77

Table 3: Results (Accuracy %) on FER task, using different labels (*smiling* and *hair color*) in Purified Learning.

¹Link to Paperwithcode

Datasets and Feature Extractors In the digit recognition experiments, regarding *background color* as the task-irrelevant features, we also use a small-scale training set, which are 20000 pictures selected from MNIST (LeCun et al. 1998). The test sets are SVHN (Netzer et al. 2011) and MNIST-M (Ganin et al. 2016). The two groups of samples are randomly sampled from MNIST and the combination of MNIST and SVHN respectively. Besides, all pictures are converted to RGB pictures and we use 32×32 resolution for them. The datasets used in the experiment are detailed in Appendix C.

Additionally, we select ResNet18 (He et al. 2016), Vg-Net11 (Simonyan and Zisserman 2015), DenseNet121 (Huang et al. 2017), SeNet (Hu, Shen, and Sun 2018), EfficientNet (Tan and Le 2019), MobileNetV2 (Sandler et al. 2018) and ShuffleNetV2 (Ma et al. 2018) as feature extractors.

Results Table 2 is the comparison between our method and two baselines. Compared with baselines, Purified Learning achieves higher accuracy than DANN and Goal 1 Only method. The Although transferring from MNIST to SVHN is difficult since SVHN is much more complex than MNIST, Purified Learning improves DANN by more than 10% accuracy, which proves the effectiveness of using task-irrelevant features. We also achieve better results than DANN in the “MNIST to MNIST-M” task.

Discussion

The impact of different levels of task-irrelevance. As different task-relevance can affect the performance of transfer learning, it is essential to study the impact of different levels of task-irrelevance on Purified Learning. Except for the *hair color* label, we use the *smiling* label from CelebA. We apply these labels to the Purified Learning framework and compare their performance.

Table 3 indicates that the experiment results that compared with Goal 1 Only method, the performance of Purified Learning remains the same or gets worse when using the *smiling* label, but have significant improvement when using the *hair color* label. The experiment results suggest that using a more irrelevant label is better for the Purified Learning framework to improve the performance since it tries to use the knowledge of task-irrelevant features. On the other hand, if we misuse task-relevant samples in Purified Learning, it will have a negative impact. This is similar to negative transfer while using task-irrelevant labels in transfer learning. In general, this phenomenon means that Purified Learning differs from transfer learning, since it benefits from the irrelevance of data instead of relevance.

PCA analysis on feature representations Based on the maximum variance theory (Tipping and Bishop 1999), if the percentage of variance explained by principal components increase, the representation vector will contain more information about task-relevant features, and task-relevant information will be better retained during the process of dimension reduction. Due to the limitation of paper length, we only show the results of ResNet18 as an example, the rest of them are listed in Appendix D.

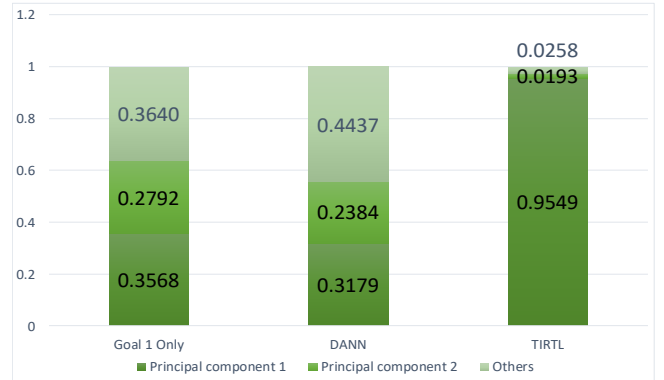


Figure 2: PCA results of ResNet18 on digit recognition task. The larger the proportion of the dark green part (principal component 1 & 2), the larger the proportion of the components that are decisive to the task in the representation.

Figure 2 shows the proportion of principal components of different methods in digit recognition tasks. Compared with other methods (Goal 1 Only and DANN), the proportion of task-relevant information is significantly higher in Purified Learning, which means that Purified Learning learns knowledge from task-irrelevant labels and avoid extracting task-irrelevant features during feature extraction.

Feature Extractor	Train \rightarrow Test Dataset	Goal 1 Only	PL (Hair Color)	TL (Expression)	TL (Expression + PL (Hair Color))
AlexNet	ck+ \rightarrow mmi	35.91	37.61	60.71	61.98
	ck+ \rightarrow oulu	34.75	38.31	51.64	53.31
	mmi \rightarrow ck+	56.36	61.45	79.88	81.82
	mmi \rightarrow oulu	22.12	22.61	51.92	52.06
	oulu \rightarrow ck+	55.03	59.64	82.67	83.39
	oulu \rightarrow mmi	39.46	45.36	56.70	59.70
ResNet34	Average	40.61	44.16	63.92	65.36
	ck+ \rightarrow mmi	50.42	50.42	58.52	59.53
	ck+ \rightarrow oulu	50.94	51.78	64.62	64.62
	mmi \rightarrow ck+	65.33	69.21	79.27	80.00
	mmi \rightarrow oulu	44.87	42.43	60.64	60.57
	oulu \rightarrow ck+	73.45	80.12	85.45	86.42
VggNet19	oulu \rightarrow mmi	54.13	54.30	65.43	67.12
	Average	56.52	58.04	68.99	69.71
	ck+ \rightarrow mmi	45.53	45.53	61.21	66.61
	ck+ \rightarrow oulu	56.66	57.22	61.27	61.13
	mmi \rightarrow ck+	65.33	66.79	81.33	82.79
	mmi \rightarrow oulu	45.08	46.76	59.46	59.73
	oulu \rightarrow ck+	76.73	78.91	86.18	90.18
	oulu \rightarrow mmi	45.03	51.43	58.68	60.20
	Average	55.73	57.77	68.02	70.11

Table 4: Results (Accuracy %) of the combined model on FER task. TL (Expression) + PL (Hair Color) refers to a combined model using both task-relevant and task-irrelevant labels.

Combining Purified Learning with Other Methods Above experiments demonstrate that Purified Learning utilizes task-irrelevant samples to improve the target learner, while many existing methods such as transfer learning use task-relevant samples to achieve the same goal. This prompts us to consider combining both task-relevant and

task-irrelevant samples to obtain better performance. Due to the scalability and flexibility of Purified Learning, it can be integrated easily with existing methods. Specifically, we pre-train the model on a large FER dataset, RAF (Li, Deng, and Du 2017a), and then fine-tune it on a small-scale training dataset with Purified Learning. Table 4 indicates that although task-relevant transfer learning brings great performance improvement itself, combining with the Purified Learning framework can yield better performance of model generalization.

Conclusion

In this paper, we propose a novel framework, Purified Learning, to exploit the knowledge from additional task-irrelevant labels in order to solve the problem caused by the unreliable empirical risk minimization when the training dataset is small. Based on detailed theoretical analysis, we illustrate that samples with task-irrelevant labels can be used in improving the generalization performance of the model, based on which we propose Purified Learning, which directly obtains and utilizes knowledge from a wide range of task-irrelevant labels. Furthermore, Purified Learning can be well combined with the existing task-relevant learning methods. We believe that the exploration of task-irrelevant labels in our work provides a valuable insight for future research.

References

Ajakan, H.; Germain, P.; Larochelle, H.; Laviolette, F.; and Marchand, M. 2014. Domain-adversarial neural networks. *arXiv preprint arXiv:1412.4446* .

Ajiboye, A.; Abdullah-Arshah, R.; and Hongwu, Q. 2015. Evaluating the effect of dataset size on predictive model using supervised learning technique .

Arbelaez, P.; Maire, M.; Fowlkes, C.; and Malik, J. 2010. Contour detection and hierarchical image segmentation. *IEEE transactions on pattern analysis and machine intelligence* 33(5): 898–916.

Arjovsky, M.; Chintala, S.; and Bottou, L. 2017. Wasserstein gan. *arXiv preprint arXiv:1701.07875* .

Bowles, C.; Chen, L.; Guerrero, R.; Bentley, P.; Gunn, R.; Hammers, A.; Dickie, D. A.; Hernández, M. V.; Wardlaw, J.; and Rueckert, D. 2018. Gan augmentation: Augmenting training data using generative adversarial networks. *arXiv preprint arXiv:1810.10863* .

Caruana, R. 1993. Multitask Learning: A Knowledge-Based Source of Inductive Bias. In *Proceedings of the Tenth International Conference on Machine Learning*, 41–48. Morgan Kaufmann.

Chen, T.; Kornblith, S.; Norouzi, M.; and Hinton, G. 2020. A simple framework for contrastive learning of visual representations. *arXiv preprint arXiv:2002.05709* .

Cubuk, E. D.; Zoph, B.; Mane, D.; Vasudevan, V.; and Le, Q. V. 2018. Autoaugment: Learning augmentation policies from data. *arXiv preprint arXiv:1805.09501* .

Ganin, Y.; and Lempitsky, V. 2015. Unsupervised domain adaptation by backpropagation. In *International conference on machine learning*, 1180–1189. PMLR.

Ganin, Y.; Ustinova, E.; Ajakan, H.; Germain, P.; Larochelle, H.; Laviolette, F.; Marchand, M.; and Lempitsky, V. 2016. Domain-adversarial training of neural networks. *The Journal of Machine Learning Research* 17(1): 2096–2030.

Gu, J.; Wang, Z.; Kuen, J.; Ma, L.; Shahroud, A.; Shuai, B.; Liu, T.; Wang, X.; Wang, G.; Cai, J.; et al. 2018. Recent advances in convolutional neural networks. *Pattern Recognition* 77: 354–377.

He, K.; Zhang, X.; Ren, S.; and Sun, J. 2016. Deep residual learning for image recognition. In *Proceedings of the IEEE conference on computer vision and pattern recognition*, 770–778.

Hu, J.; Shen, L.; and Sun, G. 2018. Squeeze-and-excitation networks. In *Proceedings of the IEEE conference on computer vision and pattern recognition*, 7132–7141.

Huang, G.; Liu, Z.; Van Der Maaten, L.; and Weinberger, K. Q. 2017. Densely connected convolutional networks. In *Proceedings of the IEEE conference on computer vision and pattern recognition*, 4700–4708.

Krizhevsky, A.; Sutskever, I.; and Hinton, G. E. 2012. ImageNet Classification with Deep Convolutional Neural Networks. In Pereira, F.; Burges, C. J. C.; Bottou, L.; and Weinberger, K. Q., eds., *Advances in Neural Information Processing Systems 25*, 1097–1105. Curran Associates, Inc. URL <http://papers.nips.cc/paper/4824-imagenet-classification-with-deep-convolutional-neural-networks.pdf>.

LeCun, Y.; Bottou, L.; Bengio, Y.; and Haffner, P. 1998. Gradient-based learning applied to document recognition. *Proceedings of the IEEE* 86(11): 2278–2324.

Li, S.; Deng, W.; and Du, J. 2017a. Reliable crowdsourcing and deep locality-preserving learning for expression recognition in the wild. In *Proceedings of the IEEE conference on computer vision and pattern recognition*, 2852–2861.

Li, S.; Deng, W.; and Du, J. 2017b. Reliable Crowdsourcing and Deep Locality-Preserving Learning for Expression Recognition in the Wild. In *2017 IEEE Conference on Computer Vision and Pattern Recognition (CVPR)*, 2584–2593. IEEE.

Liu, Z.; Luo, P.; Wang, X.; and Tang, X. 2015. Deep Learning Face Attributes in the Wild. In *Proceedings of International Conference on Computer Vision (ICCV)*.

Lucey, P.; Cohn, J. F.; Kanade, T.; Saragih, J.; Ambadar, Z.; and Matthews, I. 2010. The extended cohn-kanade dataset (ck+): A complete dataset for action unit and emotion-specified expression. In *2010 ieee computer society conference on computer vision and pattern recognition workshops*, 94–101. IEEE.

Luo, Z.; Zou, Y.; Hoffman, J.; and Fei-Fei, L. F. 2017. Label efficient learning of transferable representations across domains and tasks. In *Advances in Neural Information Processing Systems*, 165–177.

Ma, N.; Zhang, X.; Zheng, H.-T.; and Sun, J. 2018. Shufflenet v2: Practical guidelines for efficient cnn architecture design. In *Proceedings of the European conference on computer vision (ECCV)*, 116–131.

Mohri, M.; Rostamizadeh, A.; and Talwalkar, A. 2012. *Foundations of Machine Learning*. Adaptive computation and machine learning. MIT Press. ISBN 978-0-262-01825-8.

Netzer, Y.; Wang, T.; Coates, A.; Bissacco, A.; Wu, B.; and Ng, A. Y. 2011. Reading digits in natural images with unsupervised feature learning .

Pantic, M.; Valstar, M.; Rademaker, R.; and Maat, L. 2005. Web-based database for facial expression analysis. In *2005 IEEE international conference on multimedia and Expo*, 5–pp. IEEE.

Prusa, J.; Khoshgoftaar, T. M.; and Seliya, N. 2015. The effect of dataset size on training tweet sentiment classifiers. In *2015 IEEE 14th International Conference on Machine Learning and Applications (ICMLA)*, 96–102. IEEE.

Rosenstein, M. T.; Marx, Z.; Kaelbling, L. P.; and Dietterich, T. G. 2005. To transfer or not to transfer. In *NIPS 2005 workshop on transfer learning*, volume 898, 1–4.

Sandler, M.; Howard, A.; Zhu, M.; Zhmoginov, A.; and Chen, L.-C. 2018. Mobilenetv2: Inverted residuals and linear bottlenecks. In *Proceedings of the IEEE conference on computer vision and pattern recognition*, 4510–4520.

Shen, J.; Qu, Y.; Zhang, W.; and Yu, Y. 2017. Wasserstein distance guided representation learning for domain adaptation. *arXiv preprint arXiv:1707.01217* .

Shinohara, Y. 2016a. Adversarial Multi-Task Learning of Deep Neural Networks for Robust Speech Recognition. In *Interspeech*, 2369–2372. San Francisco, CA, USA.

Shinohara, Y. 2016b. Adversarial Multi-Task Learning of Deep Neural Networks for Robust Speech Recognition. In *Interspeech*, 2369–2372. San Francisco, CA, USA.

Simonyan, K.; and Zisserman, A. 2015. Very Deep Convolutional Networks for Large-Scale Image Recognition. In *International Conference on Learning Representations*.

Tan, M.; and Le, Q. V. 2019. Efficientnet: Rethinking model scaling for convolutional neural networks. *arXiv preprint arXiv:1905.11946* .

Tipping, M. E.; and Bishop, C. M. 1999. Mixtures of probabilistic principal component analyzers. *Neural computation* 11(2): 443–482.

Tommasi, T.; Patricia, N.; Caputo, B.; and Tuytelaars, T. 2017. A deeper look at dataset bias. In *Domain adaptation in computer vision applications*, 37–55. Springer.

Torralba, A.; and Efros, A. A. 2011. Unbiased look at dataset bias. In *CVPR 2011*, 1521–1528. IEEE.

Vapnik, V. 1991. Principles of Risk Minimization for Learning Theory. In Moody, J. E.; Hanson, S. J.; and Lippmann, R., eds., *Advances in Neural Information Processing Systems 4, [NIPS Conference, Denver, Colorado, USA, December 2-5, 1991]*, 831–838. Morgan Kaufmann.

Wang, Y.; Yao, Q.; Kwok, J. T.; and Ni, L. M. 2020. Generalizing from a few examples: A survey on few-shot learning. *ACM Computing Surveys (CSUR)* 53(3): 1–34.

Wang, Y.-X.; and Hebert, M. 2016. Learning to learn: Model regression networks for easy small sample learning. In *European Conference on Computer Vision*, 616–634. Springer.

Weiss, K.; Khoshgoftaar, T. M.; and Wang, D. 2016. A survey of transfer learning. *Journal of Big data* 3(1): 9.

Yosinski, J.; Clune, J.; Bengio, Y.; and Lipson, H. 2014. How transferable are features in deep neural networks? In *Advances in neural information processing systems*, 3320–3328.

Zhang, K.; Zhang, Z.; Li, Z.; and Qiao, Y. 2016. Joint face detection and alignment using multitask cascaded convolutional networks. *IEEE Signal Processing Letters* 23(10): 1499–1503.

Zhang, X.; Wang, Z.; Liu, D.; Lin, Q.; and Ling, Q. 2020. Deep Adversarial Data Augmentation for Extremely Low Data Regimes. *IEEE Transactions on Circuits and Systems for Video Technology* .

Zhang, Z.; Luo, P.; Loy, C. C.; and Tang, X. 2014. Facial landmark detection by deep multi-task learning. In *European conference on computer vision*, 94–108. Springer.

Zhao, G.; Huang, X.; Taini, M.; Li, S. Z.; and Pietikäinen, M. 2011. Facial expression recognition from near-infrared videos. *Image and Vision Computing* 29(9): 607–619.

A. Methods on how to combine with existing models

Purified Learning can be integrated with other methods without any conflict. As shown in Figure 1 in the paper, to combine our Purified Learning with task-relevant transfer learning, the straightforward way is to perform a mature transfer learning method with task-relevant samples at first and then use Purified Learning. The combined model could be jointly optimized:

$$\mathcal{L} = \mathcal{L}_{\text{Purified Learning}} + \mathcal{L}_{\text{Others}}, \quad (27)$$

where $\mathcal{L}_{\text{Others}}$ denotes the loss of other learning methods such as transfer learning which often use task-relevant samples. Here, $\mathcal{L}_{\text{Purified Learning}}$ utilizes training samples as well as task-irrelevant samples, and $\mathcal{L}_{\text{Others}}$ utilizes training samples as well as task-relevant samples. The integrated model makes better use of the knowledge in both task-irrelevant samples and task-relevant samples, and empirical studies show that the integrated model achieves better generalization performance than solely using transfer learning.

B. Experimental implementation details

We provide implementation details of the comparison method used in our experiments.

Facial Expression Recognition

- **Transfer learning:** We adopt the pre-training and fine-tuning approach to transfer learning based on shared parameters (Yosinski et al. 2014). We first pre-train the feature extractor as well as the classifier on CelebA for hair color classification and then train the whole model on the expression dataset.
- **Multi-task learning:** We adopt the multi-task learning approach with hard parameter sharing of hidden layers (Caruana 1993). Specifically, a shared feature extractor accepts both images with hair color tags from CelebA and images with expression tags from a training set. And two independent classifier networks make separate predictions for hair color and expressions. The entire network gets trained by backpropagating the final loss which is calculated by adding up the classification loss of hair color and the classification loss of expression.
- **Adversarial Multi-task Learning:** Based on the multi-tasking learning model, a new gradient reversal layer (GRL) is added between the feature extractor and the hair color classifier, where the idea is consistent with Shinohara (Shinohara 2016b).

Digit Recognition

- **DANN:** DANN is a framework for unsupervised domain adaptation based on adversarial multitasking learning proposed by Ganin (Ganin et al. 2016). As a comparison method for the simultaneous use of MNIST and SVHN data, it is implemented by adding a new gradient reversal layer (GRL) and a domain classifier with 2-dimensional outputs for domain classification to the existing feature extractor and classifier. The feature extractor accepts both images from MNIST and SVHN. One classifier then classifies the feature representation of the MNIST data from 0 to 9, and another classifier distinguishes whether the feature representation originates from MNIST or SVHN.

C. Datasets Details

Facial Expression Recognition

- **CK+** (we use 927 images): The Extended Cohn-Kanade (CK+) dataset has the facial behavior of 210 adults was recorded using two hardware synchronized Panasonic AG-7500 cameras. Participants were 18 to 50 years of age, 69% female, 81%, Euro-American, 13% Afro-American, and 6% other groups (Lucey et al. 2010). CK+ is available at <http://www.consortium.ri.cmu.edu/ckagre/>.
- **Oulu** (we use 1440 images): The Oulu Multi-pose Eye Gaze Dataset includes 200 image sequences from 50 subjects (For each subject it includes four image sequences). Each sequence consists of 225 frames captured when people are fixating on 10 targeting points on the screen (Zhao et al. 2011). Oulu is available at <https://sites.google.com/site/oulunpudatabase/>.
- **MMI** (we use 639 images): The MMI Facial Expression Database, which includes more than 1500 samples of both

static images and image sequences of faces in frontal and in profile view displaying various expressions of emotion, single and multiple facial muscle activation (Pantic et al. 2005). MMI is available at <https://mmifacedb.eu/>.

- **CelebA:** CelebFaces Attributes Dataset (CelebA) is a large-scale face attributes dataset with more than 200K celebrity images, each with contains 40 attribute annotations without detailed emotion labels. It is noteworthy that there is a “smile” expression label in CelebA, but we do not use it in our experiment (Liu et al. 2015). CelebA is available at <http://mmlab.ie.cuhk.edu.hk/projects/CelebA.html>.
- **RAF:** Real-world Affective Faces Database (RAF) is a large-scale dataset of facial expressions containing approximately 30,000 diverse facial images downloaded from the Internet, where includes a 7-dimensional expression distribution vector for each image (Li, Deng, and Du 2017b). RAF is available at <http://whdeng.cn/RAF/model1.html>.



Figure 3: Examples of datasets used in the facial expression recognition experiments, which have been preprocessed through MTCNN for alignment. Notice that the characters have a more homogenous hair color (black in CK+ and brown in Oulu), while the hair color is richer in MMI. Hair is usually not visible in the task-relevant dataset RAF, whereas hair color is varied in CelebA.



Figure 4: Examples of datasets used in the digital recognition experiments. Note that MNIST contains only the black background and white numbers, while SVHN and MNIST contain a variety of colored backgrounds and numbers.

Digit Recognition

- **MNIST:** The MNIST handwritten digit database has a training set of 60,000 samples and a test set of 10,000 samples (LeCun et al. 1998). The numbers have been size-standardized to a 28×28 image size and are centered on a fixed digital center. MNIST is available at <http://yann.lecun.com/exdb/mnist/>.
- **SVHN:** The Street View House Numbers Dataset (SVHN) is a real-world image dataset (Netzer et al. 2011). It can be seen as similar in flavor to MNIST (e.g., the images are of small cropped digits), but incorporates an order of magnitude more labeled data (over 600,000 digit images) and comes from a significantly harder, unsolved, real-world problem (recognizing digits and numbers in natural scene images). SVHN is available at <http://ufldl.stanford.edu/housenumbers/>.
- **MNIST-M:** The acquisition of MNIST-M is the same as (Ganin et al. 2016). Specifically, we blend digits from the MNIST over patches randomly extracted from color photos from BSDS500 (Arbelaez et al. 2010).

D. Additional Experimental Results

Verify the correctness of the DANN implementation

The method (DANN) proposed in (Ajakan et al. 2014) to achieve unsupervised domain adaptation based on the adversarial multi-task learning framework has achieved great success and has been widely used. We found in experiments (refer to experiments on digit recognition) that it is very difficult to implement domain adaptation from MNIST to SVHN, and the DANN framework will even weaken the original performance of the model. For this reason, we add an experiment that realizes domain adaptation from SVHN to MNIST to verify the correctness of our DANN’s implementation. The experimental results are shown in Table 1.

In the additional experiment, the model using DenseNet121 as the feature extractor achieved an accuracy of 83.36 on the MNIST test dataset under the DANN framework, which is higher than the result(73.85) reported in the original paper (Ganin and Lempitsky 2015). Note that we only use 20,000 pictures from SVHN as a training dataset. The experiment also shows that the DANN framework would greatly improve some models (DenseNet121, SeNet, and ShuffleNetV2), but the improvement effect is not obvious for other models. In contrast, Purified Learning is significantly more general. Also noticed that although the average performance of Purified Learning under the MNIST test dataset is not as good as that of DANN, Purified Learning has achieved better performance on the MNIST-M test dataset. This is because DANN as a domain adaptation method focuses on improving the model in a known target domain, while Purified Learning focuses on improving the generalization performance of the model under the unseen test samples. Also, it is worth noting that the background and foreground colors of the pictures in SVHN are more evenly distributed than MNIST, which is the main reason

why the improvement effect of Purified Learning on SVHN is not obvious.

Other PCA analysis results

Due to the paper’s length limitation, we only use the results of ResNet18 as an example, and the other results are shown in Figure 5. It can be guided from Figure 5 that the results on other models are the same as our results using ResNet as an example. The proportion of task-relevant information is much higher in Purified Learning on all models, which indicates that the feature representation vectors are easier to aggregate in Purified Learning.

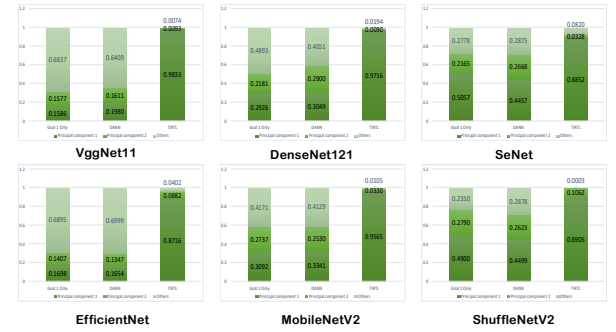


Figure 5: PCA results of other feature extractors on the digit recognition task.

Train → Test Dataset	Feature Extractor	Goal 1 Only	DANN	PL (Background Color)
SVHN → MNIST	DenseNet121	67.36	83.36	63.05
	EfficientNet	50.63	55.23	64.38
	MobileNetV2	62.50	64.20	66.99
	ResNet18	59.80	60.36	62.73
	SeNet	50.72	77.34	57.04
	ShuffleNetV2	47.52	66.60	48.94
	VggNet11	62.96	54.14	61.07
SVHN → MNIST-M	Average	57.36	65.89	60.60
	DenseNet121	39.80	44.38	40.06
	EfficientNet	35.50	35.80	46.62
	MobileNetV2	40.86	40.82	42.08
	ResNet18	35.52	35.91	40.94
	SeNet	31.14	37.34	40.48
	ShuffleNetV2	33.70	38.81	33.42
	VggNet11	43.13	41.20	42.14
	Average	37.09	39.18	40.82

Table 5: Additional results (Accuracy %) on digit recognition task.